
Design and Analysis of Diversity Based Decision Fusion in Underwater Sensor Networks Communication

Vibhav Kumar Sachan^{*a}, Shweta^a and Syed Akhtar Imam^b

^{*a}*Department of Electronics & Communication Engineering
KIET Group of Institutions, Ghaziabad, U.P, India.*

^b*Department of Electronics & Communication Engineering
Jamia Millia Islamia, New Delhi, India.*

*vibhavsachan@gmail.com

Abstract

Underwater sensor network has different applications ranging from environmental monitoring, data collection to survey mission and coastal surveillance. In this paper, we study the performance of energy detector for binary-decision fusion over a multiple access channel in underwater acoustic wireless sensor network. The paper suggests a MIMO model which includes diversity at the both transmitter and receiver side. The sub-optimal decision fusion rule over MIMO channel (diversity base) improved the numerical instability, reduced complexity and required lower system knowledge. Here, we analyzed the performance of local sensors and then describing the value of probability of false alarm and missed detection (P_f) and (P_m). The combination of these values at decision fusion centre provide global decision (q_m) and (q_f), which demonstrate the performance of energy detector by considering different parameter include sampling frequency, SNR, number of transmitting sensor and number of receiving sensor.

Keywords- Decision Fusion, Multiple-Input Multiple-Output (MIMO), Energy Detection, Underwater Sensor Network.

Introduction

A Multi Agent System is a system collected of numerous interacting intelligent agents. MA contain by the Multi Agent System can launch by launch by same host or by different hosts or combination of MAs and software agents. Multi Agent System is used to solve problems which are hard or unfeasible for an individual agent to solve. But for a Multi Agent System the two main issues are Location management & communication. Lots of Mobile agent systems have been proposed in the literature. But most existing MASs do not provide a complete, proficient or useful location management approach. Hence, there is a need of a mechanism to locate any type of mobile agent at anytime from anywhere. Communication is also a necessary component of scattered systems and this is no exception for multi-agent systems. This paper proposes the improve mechanism to locate MAs for both cases mentioned earlier as well as provide a communication mechanism between the MAs.

Hierarchical Location Management Scheme (HLMS)

Underwater sensor network is imagined to empower various applications ranging from contamination checking, oceanographic data gathering, ecological monitoring, disaster prevention, help in navigation and information collection for coastal surveillance (Akyildiz *et al.*, 2005). One of the primary issues is the efficient utilization of the underwater acoustic channel in which acoustic propagation can be delegated the time-varying multipath propagation in water. This characteristic in the nature effect tremendous Doppler spread or shifts into the transmit signal (Stojanovic *et al.*, 2009). As the aftereffect of the limited bandwidth, which relies upon both frequency and range, inter-symbol interference (ISI) occurs in underwater communication system (Catipovic *et al.*, 1990). Presently, the term channel model,

which may be denoted as physical propagation model is appropriate for system design in underwater acoustic channel (Lanbo *et al.*, 2008). However, modeling of underwater acoustic network is still a vital matter which needs facilitate consideration.

Underwater Acoustic Communication and Networking

This segment is divided into two sub area one is underwater communication and another one is networking. Now first segment might focus on point-to-point communication issues such as modulation, channel modeling, coding and equalization. Then again, second segment might focus on algorithms and protocol for networks.

Communication

The necessity of High-speed communication systems has motivated the outlining and investigation of recent techniques at the physical layer of underwater acoustic channel such as channel equalization, phase conjunction, multicarrier transmission, multiple-input multiple-output, multichannel decision feedback, iterative decoding (Walree *et al.*, 2013; Zhang *et al.*, 2012). The space-time coding and decision feedback equalization is utilized in shallow-water frequency selective channel by reviewing point to point MIMO communication in underwater. In addition, a soft-input soft-output linear equalizer is developed for simultaneous equalization of MIMO channels with Alamouti encoding at transmission side (Nordvaad *et al.*, 2006). Furthermore, spatial modulation technique in (Kilfoyle *et al.*, 2005) is outline for the execution of numerous parallel channels in underwater environment, which is utilize to enhance both reliable information rate and receive power. Differently, in (Yang *et al.*, 2007) the two famous spatial processing approaches for communication are beam-forming (of information on closely spaced receivers) and diversity combining (of information on broadly spaced receiver) is explained.

Networking

The underwater applications become more feasible when networking technologies among underwater gadgets in (Sozer, et al., 2000) must be empowered. The energy-efficient multiple access protocol which is appropriate for underwater networks has been portrayed in (Park *et al.*, 2007; Liao *et al.*, 2012). Now, the fundamental differences for example: attenuation, noise, propagation delay, useable bandwidth, transmitting power and energy consumption in underwater acoustic and terrestrial radio network were analyzed in (Zorzi *et al.*, 2008). The energy-efficient routing protocols for WSNs have been customized for underwater acoustics network in (Chen *et al.*, 2013) and (Zhang *et al.*, 2013). Power and bandwidth allocation scheme in (Jordet *et al.*, 2010) with minimum energy consumption is proposed for multi-hop underwater sensor network.

Decision Fusion

For wireless sensor network (WSN) with endless sensors, decision fusion principle utilizes the aggregate number of detection or information reported by local sensor for a final evaluation on binary hypothesis testing. Distributed detection in wireless sensor network is still a vibrant region to investigate: let us consider a scheme in which the nearby decision transmitted by the sensors to the decision fusion centre which takes a global decision by appropriate joining of the received data. Some architecture taken into account based on parallel access channels have been discussed in (Chen *et al.*, 2004; Park *et al.*, 2010): in which each sensor is orthogonal to other, channel communicate with the fusion centre. Channel state information (CSI) of optimal fusion rules is accessible at the collector is describe in (Lei *et al.*, 2010). The impact of multiple transmitter and receiver for distributed detection is examined on the basis of MIMO techniques in the terms of performance, complexity and knowledge requirement (Ciunzo *et al.*, 2012). Diagnostic results for compelling framework operating at low SNR is considered in (Ciunzo *et al.*, 2013). The performance of received-energy at decision fusion centre depends on optimal test (under Bayesian/ Neyman-person approach) over Rayleigh fading channel is presented in (Ciunzo *et al.*, 2015). Further, relaxation of the perfect coherent detection assumptions and related framework is design in (Xu *et al.*, 2013). Finally, the distributed detection fusion in which scan statistic is exploited for active

detection in underwater network is explained in (Lee *et al.*, 2014). To best of our insight, Diversity base decision fusion in underwater situation is still unexplored.

Paper Organization

The fundamental contribution of this paper is energy detection for diversity base decision fusion in underwater acoustic channels. Distributed underwater sensors spread a signal if an event of significance is acknowledged locally, i.e. we are of the view on-off keying (OOK) modulation. An array receiver fuses the signals utilizing energy detection from the numerous sensors, i.e. the energy got from various sensors is the statistics for the binary decision on the event of an occasion in the area observed by the network. We expect a binary source, which makes the work adequate for applications, For example: threshold-based occasion detection. Its merits seeing that (Song *et al.*, 2012) investigated with regards to distribution detection, OOK is used as frequency shift keying (FSK). It is demonstrated that OOK save more energy that of FSK but exhibits blunder execution. However, the work acknowledges parallel channels to the fusion centre, while our work concentrates on interfering channels.

For ordinary underwater acoustic channels, at one case the optimal rule for decision fusion is not realistic (as in most situations), however another instance is that the fusion rule based on energy detection is suboptimal because of the way that the channel measurements mismatch the Rayleigh fading model. Here we investigate the effect on the performance of different designed parameters for example: SNR, pulse duration, integration time, sampling frequency, sampling frequency, sensor quality, number of transmitting sensors and number of receiving element (hydrophone). Likewise, we show up a sensible setup can approach the optimum execution in a realistic circumstance. The fundamental favorable circumstances of the present system are:

- it does not require idealize synchronization;
- it does not require either channel estimation for instantaneous CSI or statistical CSI;
- it does not require knowledge of either local sensor execution or SNR;
- it is energy efficient, as it utilizes OOK;
- it accomplishes excellent execution, even with low-quality sensors;

It signifies that the energy detector is very insensitive to Doppler effects, which severely degrades performance of underwater communication systems. Moreover, underwater sensor networks are by and large in view of short-range low-power communication, so it can be considered that OOK modulation is energy proficient, if one of the two hypotheses are altogether less probable than alternate (this is basic in observing applications for anomaly detection) (Kanchumurthy *et al.*, 2008)

The layout of the paper is revolving around: in Sec. 2 we exhibit the system model; in sec 3 we investigate the measurements for the decision at the fusion centre and the figures for system execution; sec 4 gives the result and simulation of the system; finally, sec 5 highlights the conclusion remarks.

Notation: Lower- case bold letter denote vectors, with a_n denoting the nth element of \mathbf{a} ; upper-case bold letters denote matrices, with $A_{n,m}$ denotes the (n, m) the element of \mathbf{A} ; \mathbf{I}_N denotes the $N \times N$ identity matrix; $\mathbf{0}_N$ denotes the N-length vector whose element are 0; $\mathcal{D}(\cdot)$ denoting the Diract function; $E(\cdot)$, $(\cdot)^t$, and $\|\cdot\|$ denote expectation, transpose and Frobenius norm operation; $(A_1^t, \dots, A_N^t)^t$ denotes the vertical concatenation of N matrices; $\Pr(A)$ denotes the probability of the event A; $p(a)$ denotes the probability density function of the random variable a; $[a]$ denotes the largest integer value smaller than or equal to a; $R(a)$ and $j(a)$ denote the real and imaginary parts of a, respectively; j is the imaginary unit; A^n denotes the nth Cartesian power of the set A; $\sim N_c(\mathbf{\mu}, \mathbf{\Sigma})$ means "distributed according to proper complex normal distribution with mean $\mathbf{\mu}$ and $\mathbf{\Sigma}$ covariance".

System Model

In this section, as appeared in fig 1, we briefly describe the system model. Here we considered a

distributed binary hypothesis test, where K sensors sense autonomously the environment. The sensors are discriminate between the two-hypothesis denoted H_0 and H_1 and the corresponding a-prior probabilities ρ_0 and ρ_1 , respectively. We assume that the quality of the local sensors and decision process of the sensors is characterized by the local probability of false alarm $P_f(k)$ and the local probability of missed detection $P_m(k)$ for the k th sensor, both assumed to be stationary and conditionally independent given to particular hypothesis.

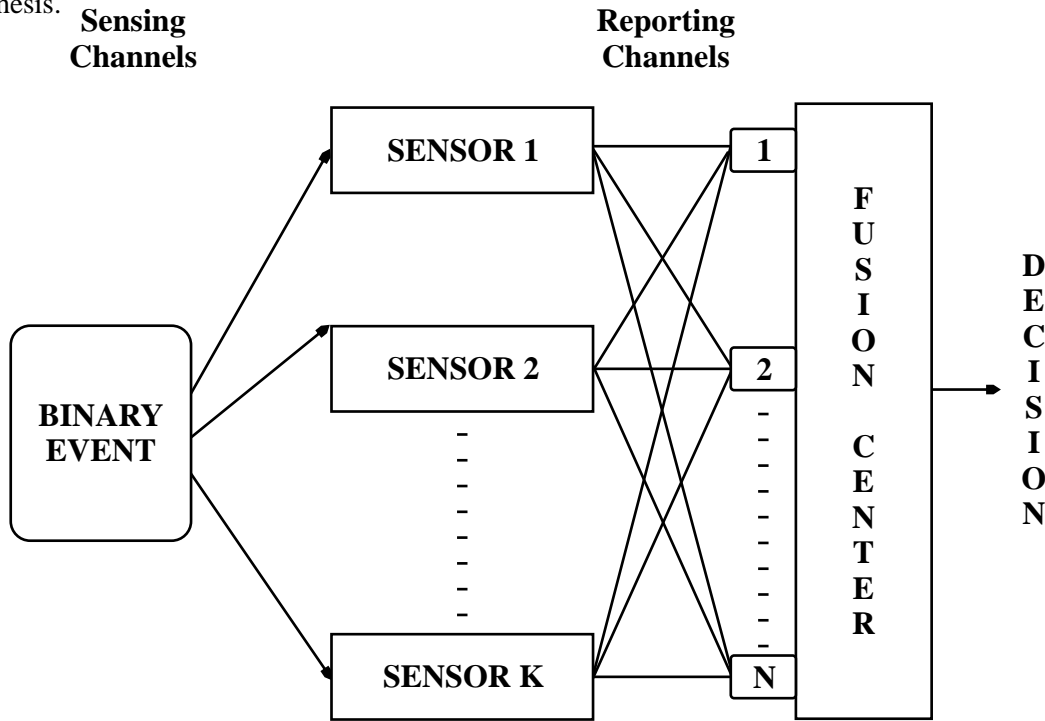


Figure 1: System Model: a binary decision with K sensors transmit signals to Fusion centre with N hydrophones

Sensors, each with one single acoustic transducer (projector), transmitted signal to the decision fusion centre, in which no dedicated channel is required to the single sensor. Further, the multiple received data of N hydrophone provide robust decision based on numerous received data. Now, for energy saving purpose the OOK modulation is utilized, in which all sensor employ the same binary modulation with parameters such as transmission pulse, carrier frequency, integration time etc.

Now, we consider a time-varying multipath channel which may be referred as multiscale multilag channel model in (Lanbo, et al., 2008) and represents a good candidate for wideband underwater acoustic channel. We will consider the following assumption as in (Walree, et al., 2013; Li, et al., 2009):

- The amplitudes are constant within one or more transmission i.e. $a_l^{(n,k)}(t) = a_l^{(n,k)}$;
- The delays are expressed in the form $\tau_l^{(n,k)}(t) = \tau_l^{(n,k)} - j_l^{(n,k)}$;
- Here, we assume 0 for H_0 and 1 for H_1

Where : $a_l^{(n,k)}(t)$ = attenuation,

$\tau_l^{(n,k)}(t)$ = Initial dealy,

$j_l^{(n,k)}(t)$ = Doppler rate, (the ratio between the relative speed of transmitter/receiver and the speed of

sound) of the (n, k) th link (channel between the projector of the k th sensor and the n th hydrophone at fusion centre), L is the maximum number resolving path for over all set of $(N \times K)$ Links.

Discrete-Time Signal Model

The m th sample of the received signal after sampling is given as

$$y[m] = \sum_{k=1}^K H_{n,k}[m] x_k + w_n[m], \tag{1}$$

Sampling with frequency f_s where:

$$y_n[m] = y_n(m/f_s), w_n[m] = w_n(m/f_s), \text{ and}$$

$$H_{n,k}[m] = \sum_{l=1}^L a_{l(n,k)} e^{-j2\pi f_c \tau_{l(n,k)}} e^{j2\pi f_l(n,k)m} \frac{fc}{f_s} \times g \left(\left(1 + f_{l(n,k)}\right) \frac{m}{f_s} - \tau_{l(n,k)} \right) \tag{2}$$

The above equation demonstrated as received signal with the noise and the channel coefficient, individually. Now, $y[m] = (y_1[m], \dots, y_N[m])'$ define as at N hydrophones, the vector combination of the signal at the m th sampling time, $w[m] = (w_1[m], \dots, w_N[m])' \sim N_c(0_N, S^2 w_{I_N})$ defines the related noise contribution $x = (x_1, \dots, x_k)'$ is the local decision from all the k sensors, and at m th sampling time, the channel matrix is defined as

$$H[m] = \begin{pmatrix} H_{1,1}[m] & \dots & H_{1,k}[m] \\ \vdots & \ddots & \vdots \\ H_{N,1}[m] & \dots & H_{N,k}[m] \end{pmatrix}, \tag{3}$$

After concluded the above equation at m th sampling time the discrete-time model for the received signal is given as

$$y[m] = H[m] x + w[m] \tag{4}$$

Now, the total time taken to collect signals is defined as an integration time T_0 , given as $M = [f_s T_0]$ successive sampling times as

$y = (y[1]', \dots, y[M]')$, $w = (w[1]', \dots, w[M]')$, $H = (H[1]', \dots, H[M]')$ offer the subsequent discrete-time model.

$$y = Hx + w \tag{5}$$

The link SNR is defining as

$$SNR = \frac{1}{S_w^2}, \tag{6}$$

The above equation show the channel condition, which is measured as proportion between the unitary energy of the active symbol and the noise variance.

Decision Fusion

The resultant decision obtained at fusion centre is generally perform a test by comparing a signal-dependent statistic ($I(y)$) and a fixed threshold (\mathcal{G}).

$$I(y) \begin{pmatrix} \tilde{H} = H_1 \\ \geq \mathcal{G} \\ \tilde{H} = H_0 \end{pmatrix} \tag{7}$$

Where H signifies the estimated hypothesis.

The performance can be calculated on the basis of the global probability of false alarm (q_f) and global

probability of missed detection (q_m), given as follows

$$q_f = pr(l(y) > \mathcal{G}H_0), \tag{8}$$

$$q_m = pr(l(y) > \mathcal{G}H_1), \tag{9}$$

The system error can be obtained as the global probability of error (q_e), discussed as follows

$$q_e = \rho q_f + \rho q_m \tag{10}$$

The threshold in Eq. (7) has been chosen in such a way that it will minimize the error probability (according to Bayes criterion (Berger *et al.*, 2009) or to provide a target probability of false alarm (according to the Neyman –person criterion (Berger *et al.*, 2009). The system execution can be obtained at complementary receiver operating characteristic (CROC) by examining the behavior of the global probability of missed detection (q_m), versus the global probability of false alarm (q_f). The optimal test (under both Bayesian/Neyman-Person) gives the log-likelihood ratio (LLR) of the obtained signal under the two hypotheses.

$$l(y) = \log \left(\frac{p(y|H1)}{p(y|H0)} \right)$$

$$l(y) = \log \left(\frac{\mathbb{E}_H \{ \hat{a} x \mathcal{E}^k p(y|H,x) \tilde{O}_{k=1}^k Pr(x_k|H_1) \}}{\mathbb{E}_H \{ \hat{a} x \mathcal{E}^k p(y|H,x) \tilde{O}_{k=1}^k Pr(x_k|H_0) \}} \right)$$

$$l(y) = \log \left(\frac{\hat{a} x \mathcal{E}^k \mathbb{E}_H \left\{ e^{-\frac{\|y-Hx\|^2}{S^2w}} \right\} \tilde{O}_{k=1}^k Pr(x_k|H1)}{\hat{a} x \mathcal{E}^k \mathbb{E}_H \left\{ e^{-\frac{\|y-Hx\|^2}{S^2w}} \right\} \tilde{O}_{k=1}^k Pr(x_k|H0)} \right) \tag{11}$$

Nevertheless, several difficulties in optimal test:

- Computationally costly (complexity is exponential with k).
- High knowledge requirement of H, P(x/Hi) and σ_w^2
- Numerically instability of the function, due to presence of exponential function (Ciuonzo *et al.*, 2015).

On account on OOK, a typical less complex option is obtained by removing the LLR with the energy of the received signal,

$$l(y) = \|y\|^2 \tag{12}$$

Which obviously requires minimal computational complexity, furthermore has the point of preference that neither CSI nor SNR nor local sensor execution required. Such an analysis has been turned to be optimal in Rayleigh fading scenarios (Kay *et al.*, 1998). This shows that the above test is also suitable in underwater acoustic channels. The execution accomplished in the ideal case that the reporting channel is perfect. The estimation bound is computed as follows,

$$q_f = \hat{a} \prod_{l=c}^k \binom{k}{l} p_f^l (1 - p_f)^{k-l} \tag{13}$$

$$q_m = \sum_{l=0}^{c-1} \binom{c-1}{l} (1 - p_m)^l p_m^{c-l} \tag{14}$$

Where: $c \in \{0, \dots, K\}$ = discrete threshold

Now, Equation (13) - (14) may be generalized, but the closed-form expression is generally intractable (especially for large K) (Li *et al.*, 2011).

Results

In this section, we verify and analyze the theoretical results obtain in section 2 and 3. Numerical results refer to Monte Carlo simulation with 104 runs using MATLAB. We have scenario based on binary event with a-priori probabilities $p_0 = 0.6$ and $p_1 = 0.2$. Up to $K=50$ transmitting sensors have been considered, whose local sensing performance has been chosen among following set: $p_f = \{0.5, 0.1, 0.15\}$ and $p_m = \{0.2, 0.4\}$.

In the presented simulation situation the various set of parameters is considered in Table 1, which are related to those assume in [9], where the accompanying “default” parameters are assumed: $K=25$ transmitting sensors, $N = 1$ hydrophone, local performance $P_f = 0.1$ and $P_m = 0.4$, SNR = -25dB sampling frequency $f_s = 2$ kHz, integration time $T_o = 12$ ms pulse duration and average inter-arrival time $\Delta = 2$ ms. Here, the simulations were matched with test in the Indian Ocean at water profundity or depth of 15 m. Now, distance between the transmitting and receiving elements is 60 to 1000 m respectively. If the value of integration time $T_o = 12$ ms is considered and the accuracy of positioning the sensor with respect to fusion centre not supposed to be exceed few meters, i.e. smaller than 15m, which is also known as negligible synchronism effect provides efficient results, although resynchronization on a regular basis may be needed (e.g. due to sound speed fluctuations).

Table 1: parameter considered in given scenario for simulation. Bold face numbers signify the default values

Name	Symbol	Value
Number of sensors	K	{15.... 2550}
Carrier frequency	f_c	13 kHz
Pulse duration	T_p	{0.5, 0.75, 1 , 1.25, 1.5, 1.75, 2}ms
Local false alarm probability	P_f	{0.05, 0.1 , 0.15}
Local miss detection probability	P_m	{0.2, 0.4 , 0.6}
Number of paths	L	12
Velocity standard deviation	V	1 m/s
Average inter-arrival Time	Δ	{1, 2 , 3}ms
Number of hydrophone	N	{ 14}
Sampling frequency	f_s	{1.5, 2 , 3}kHz
Integration time	T_o	{3, 6, 12 , 18, 24, 30}ms
SNR	SNR	{-35, -25 , -15}dB

Sensors transmit a carrier frequency $f_c = 13$ kHz and unitary- energy rectangular baseband pulse with duration $T_p = \{0.75, 1, 1.25\}$ ms is assumed. The NK links among the K projectors and N hydrophones are assumed autonomous and identically distributed. On every connection, channel coefficients have been randomly created by following these specifications:

- Here, the inter-arrival time with mean $\Delta = \{1, 2, 3\}$ ms is being exponentially distributed over

discrete number of path $L = 10$;

- Delay at various hydrophones is created by zero-mean Gaussian distribution with standard deviation d/c , where it statistically independent with respect to sensors (k) while not with respect to the hydrophones (n);(where, $d = 5$ m the approximate size of the receive array, $c = 1500$ m/s and the speed of sound in water)

The average power is exponentially decreases with delay at amplitude, where amplitudes are Rayleigh distributed with (6 dB over 10 ms);

Gaussian distribution with zero mean and standard deviation v/c provides sampled value of Doppler rates; (Where: $v = 1$ m/s the velocity related to the fusion centre and the scattered in the environment).

Up to $N = 4$ hydrophones are considered at the fusion center which may be operating with sampling frequency and integration time chosen among the following sets: $f_s = \{1.5, 2, 3\}$ kHz, $T_0 = \{6, 12, 18\}$ ms. Here, we assumed the three different SNRs, i.e. $SNR = \{-35, -25, -15\}$ dB.

SNR: Now, the figure. 2 explain the effect of SNR. The obvious change with SNR is evident. The decrease in the global probability of missed detection from $q_m = 0.052$ to $q_m = 0.018$ at global probability of false alarm $q_f = 0.05$ can be achieved by moving from $SNR = -25$ dB to $SNR = -15$ dB. This may asses the sensitivity with respect to the SNR, when $K=25$ with $P_f = 0.1$ and $P_m = 0.4$. The operation point of the single sensor, i.e. the local sensing performance (P_r, P_m) is also shown in the plot for comparison purpose.

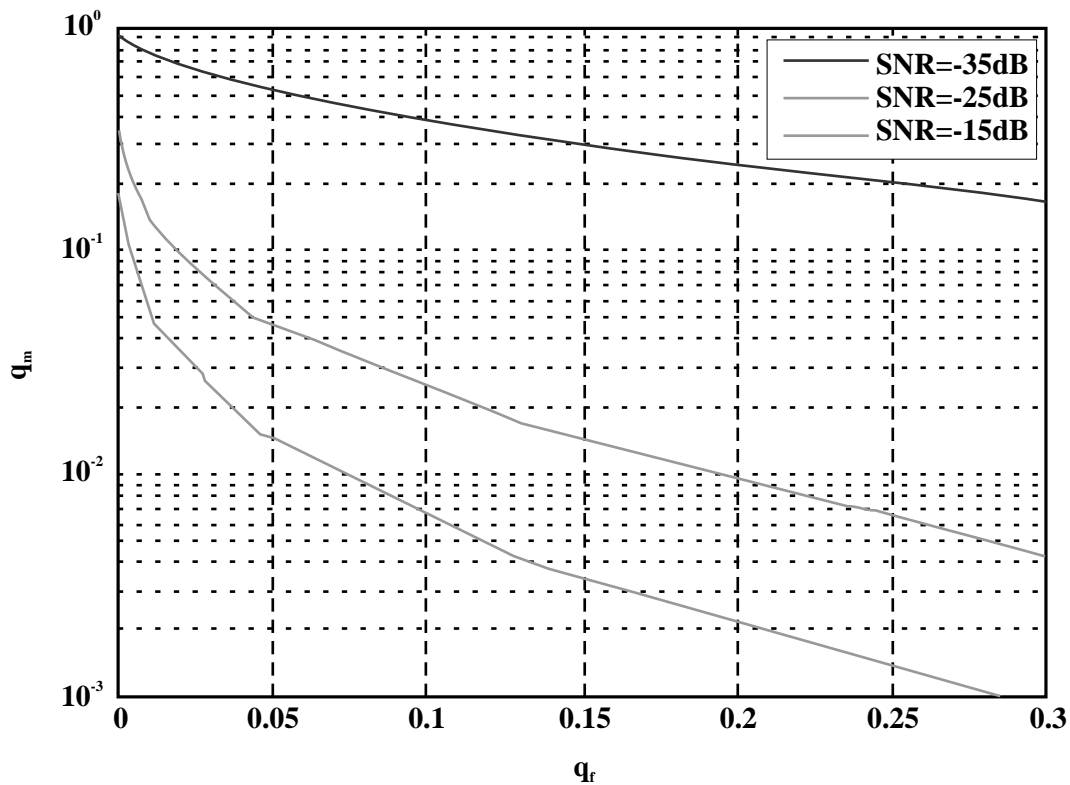


Figure 2: Impact of the SNR on the CROC with $K=25$ transmitting sensor, each with $P_f = 0.1$ and $P_m = 0.4$ and pulse duration $T_p = 1$ ms and $N = 1$ hydrophone at the fusion centre, operating with sampling frequency $f_s = 2$ Hz and integration time $T_0 = 12$ ms.

SNR: Now, the figure. 3 explain the effect of SNR. The obvious change with SNR is evident. The decrease in the global probability of missed detection from $q_m = 0.92$ to $q_m = 0.068$ at global probability of

false alarm $q_f = 0.05$ can be achieved by moving from SNR = -25 dB SNR = -15 dB. This may asses the sensitivity with respect to the SNR, when $K=25$ with $P_f = 0.15$ and $P_m = 0.6$. The operation point of the single sensor, i.e. the local sensing performance (P_f, P_m) is also shown in the plot for comparison purpose.

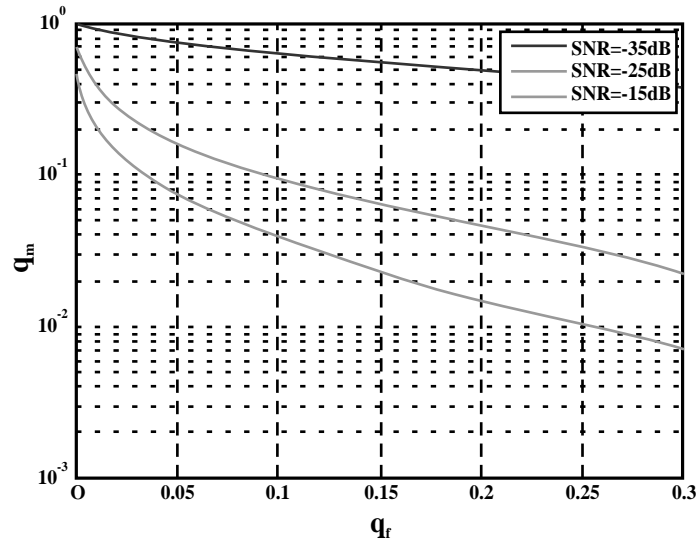


Figure 3: Impact of the SNR on the CROC with $K=25$ transmitting sensor, each with $P_f = 0.15$ and $P_m = 0.6$ and pulse duration $T_p = 1$ and $N = 1$ hydrophone at the fusion centre, operating with sampling =frequency $F_s = 2$ kHz and integration time $T_0 = 12$ ms.

Local Performance: Figure. 4 indicate the effect of local sensor performance (P_f, P_m) on CROC curve. The change in both P_f and P_m is evident. The decrease in global probability missed alarm from $q_m = 0.17$ to $q_m = 0.02$ at global probability of false alarm $q_f = 0.05$ can be achieved by moving from $P_f = 0.15$ to $P_f = 0.1$ (with fixed $P_m = 0.4$) this may asses the sensitivity with respect to P_f . Again, the decrease in global probability missed alarm from $q_m = 0.02$ to $q_m = 0.0019$ at global probability of false alarm $q_f = 0.05$ can be achieved by moving from $P_m = 0.6$ to $P_m = 0.4$ (with fixed $P_f = 0.1$) this may asses the sensitivity with respect to P_m .

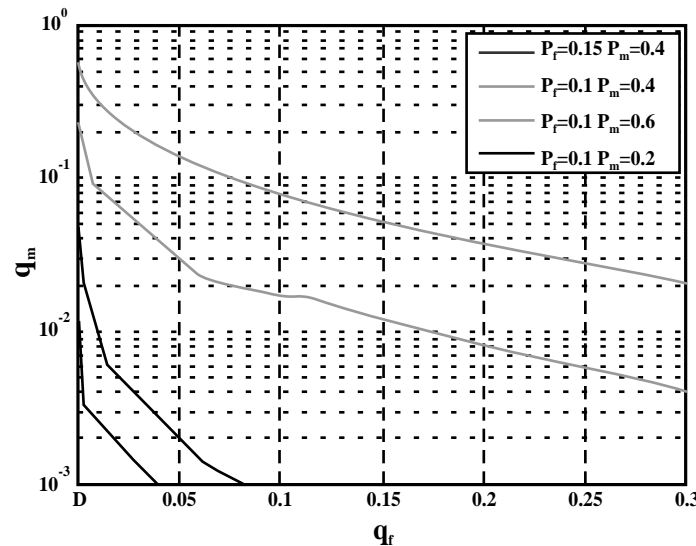


Figure 4: Impact of the local sensor performance (P_f, P_m) on the CROC with $K=25$ transmitting sensor,

each with pulse duration $T_p = 1$ ms and $N = 1$ hydrophone at the fusion centre, operating at $SNR = -25$ with sampling frequency $f_s = 2$ kHz and integration time $T_0 = 12$ ms.

Sampling Frequency and Integration Time: Now the figure 5 explain the joint effect of the sampling frequency f_s and of the integration time T_0 . The decrease in global probability missed alarm from $q_m = 0.091$ to $q_m = 0.033$ and $q_m = 0.015$ at global probability of false alarm $q_f = 0.05$ with pulse duration $T_p = 1$ ms can be achieved by moving from $f_s = 1.5$ kHz to $f_s = 2$ kHz and then to $f_s = 3$ kHz this may asses the sensitivity with respect to f_s . Now, the change with f_s is evident, while the trend regards to T_0 is not monotonic: beginning from short integration time, we first experience a fast execution change with the duration, and then after an optimal duration the observed performance is gradually decrease. The same behavior can also have obtained by the various option of the pulse duration. In our opinion, the purpose behind this phenomenon is the tradeoff between two conflicting phenomena.

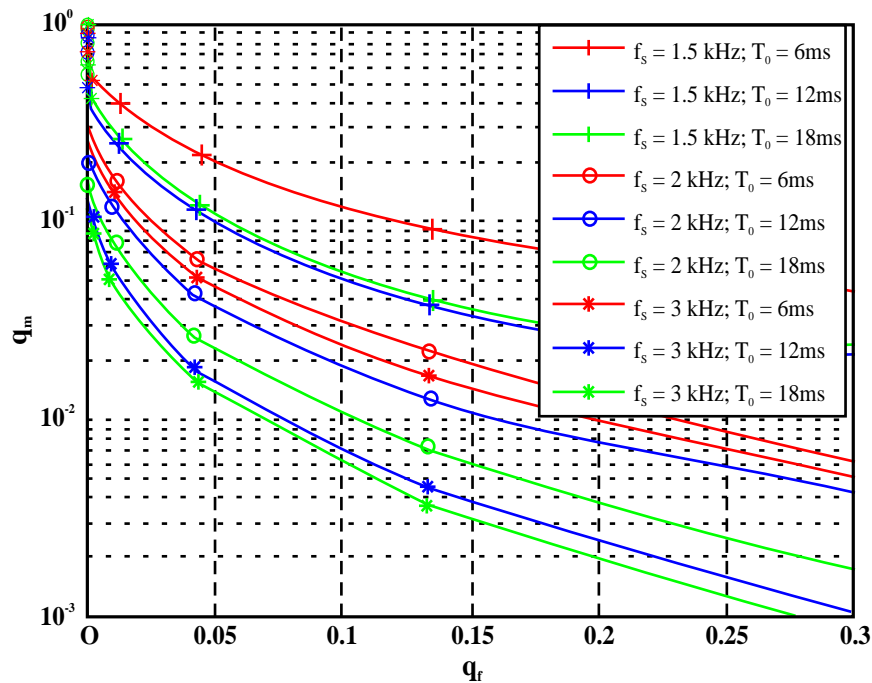


Figure 5: Impact of the sampling frequency f_s and integration time T_0 on the CROC with $K=25$ transmitting sensor, each with pulse duration $T_p = 1$ ms and $N = 1$ hydrophone at the fusion centre, operating at $SNR = -25$ with $P_f = 0.1$ and $P_m = 0.4$.

Sampling Frequency and Pulse Duration: Figure. 6 detailed the joint effect of the sampling frequency f_s and of the pulse duration T_p . The decrease in global probability missed alarm from $q_m = 0.071$ to $q_m = 0.039$ and $q_m = 0.015$ at global probability of false alarm $q_f = 0.05$ with integration time $T_0 = 12$ ms can be achieved by moving from $f_s = 1.5$ kHz to $f_s = 2$ kHz and then to $f_s = 3$ kHz this may asses the sensitivity with respect to f_s . Again, change with f_s is evident, while (analogously to the behavior with respect to T_0) the trend regards to T_p is not monotonic: beginning from short pulse duration, we first experience an execution change with the duration, and then after an optimal duration performance is gradually decreases. The same behavior can also have obtained by the various option of the pulse duration. In our opinion, the purpose behind this phenomenon is the tradeoff between two conflicting phenomena. Increasing T_p has the positive effect to allow reducing the silent intervals during the observation interval (remember that the channel response is creating different replicas of the transmitted pulse, each with different attenuation, delay and compression/expansion).

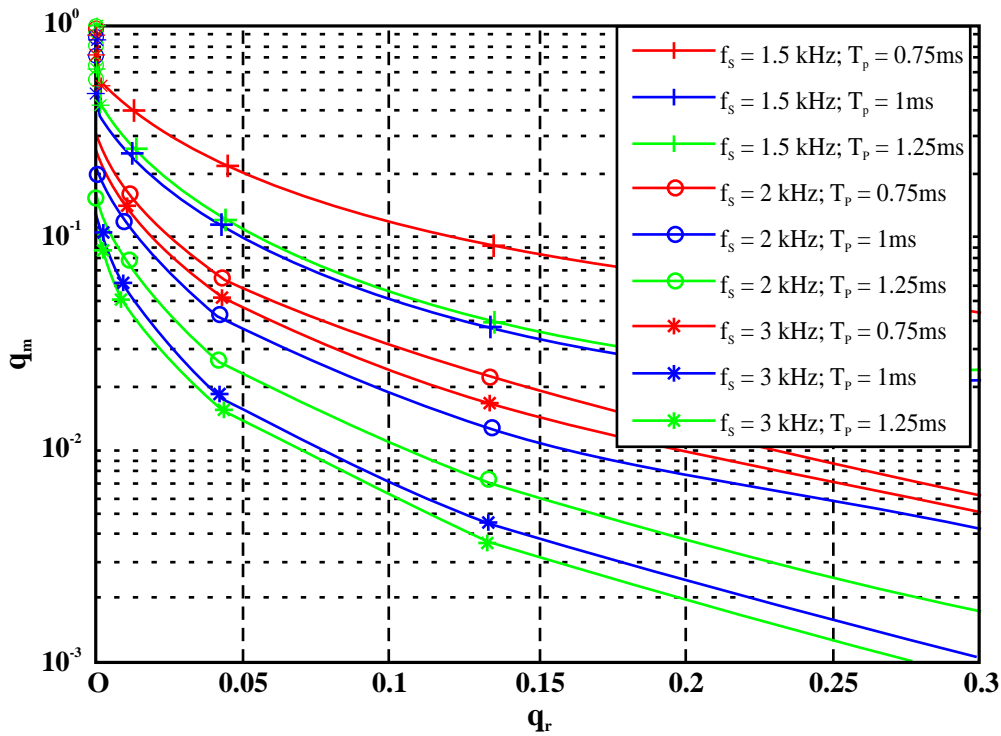


Figure 6: Impact of the sampling frequency f_s and pulse duration T_p on the CROC with $K=25$ transmitting sensor, each with integration time $T_0 = 12$ ms and $N = 1$ hydrophone at the fusion centre, operating at $SNR = -25$ with $P_f = 0.1$ and $P_m = 0.4$.

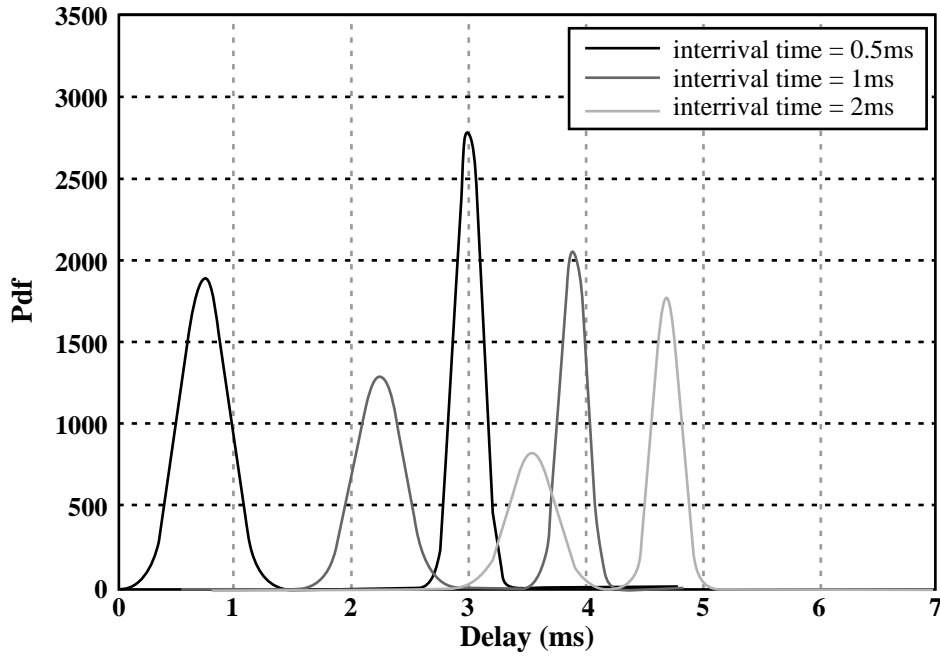


Figure 7 : Impact on \mathcal{Q} on τ_u (solid lines) and T_{rms} (dashed line)

The figure 7 illustrate the effect of three distinct values of average inter-arrival time D Ω are assumed with the related observational probability density function (pdf) of the average delay τ_u and root mean square delay spread τ_{rms} : characterized in (Varshney *et al.*, 1996). The optimum value of integration time is approx. defined as $T_0 \gg \tau_u + \tau_{rms}$ that can be obtained by different simulation of the result. It is worth noticing the fact that the energy detector is not optimal in underwater acoustic channels is confirmed by the non-monotonic behavior of the performance regarding with integration time, as including uninformative measurements can even decrease the performance. Additionally, having Rayleigh channel statistics is crucial for the derivation of the optimality of the energy detection (see Ciuonzo *et al.*, 2015).

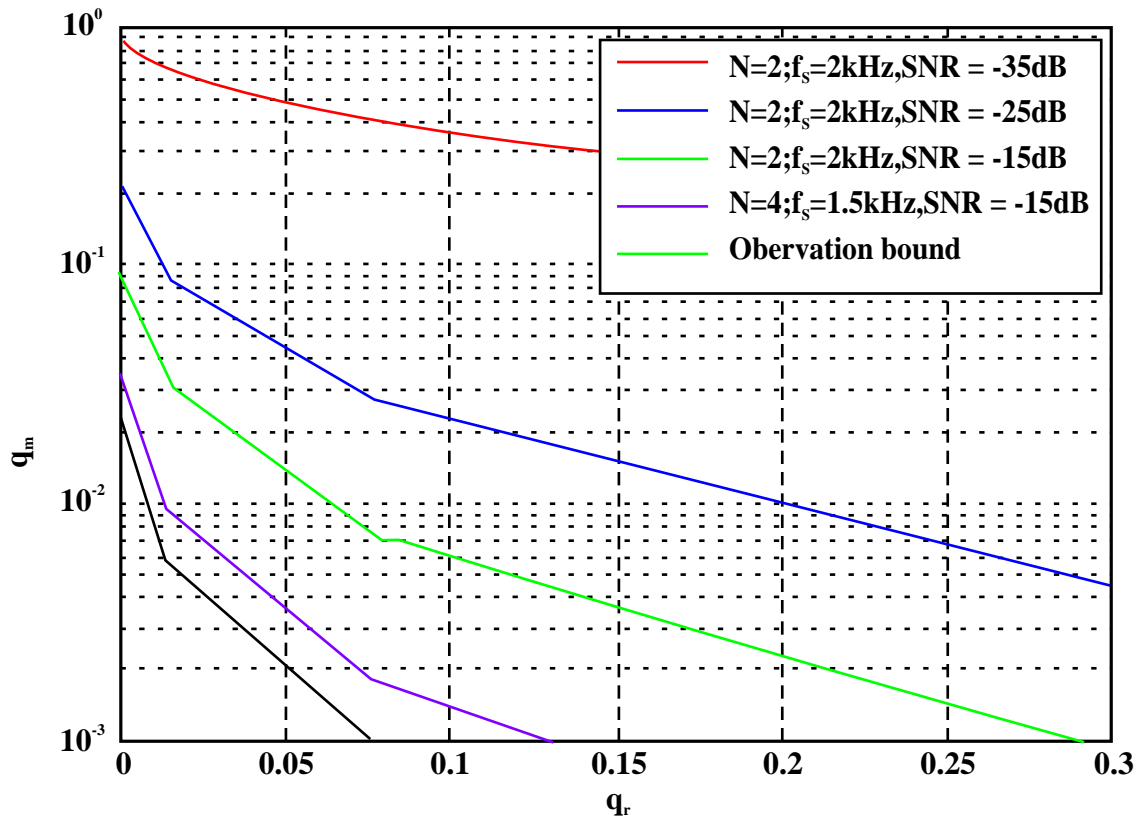


Figure 8: Approaching the observation bound with $K=25$ transmitting sensor, each with integration time $T_0 = 12$ ms and pulse duration time $T_p = 1$ ms with $P_r = 0.1$ and $P_m = 0.4$.

Now figure 8 shows CROC curves which is same appeared in figure 2 however, with two more CROC curves: one is the observation bound with parameters when $N=1$ hydrophones at the fusion centre, operating at different SNR= -15dB, SNR= -25dB and SNR= -35dB with sampling frequency $F_s = 2$ kHz, and the other one is the CROC curve in a homogeneous scenario with $N = 4$ hydrophones at the fusion center, operating at SNR = -15 dB with sampling frequency $F_s = 1.5$ kHz. Now, it is shown that the gap at $q_r = 0.1$ is such that the observation bound is $q_m = 0.0029$ while the realistic practical setup achieves $q_m = 0.0037$. This is clear how the last curve, comparing to a realistic practical setup, practically accomplished the previous curve.

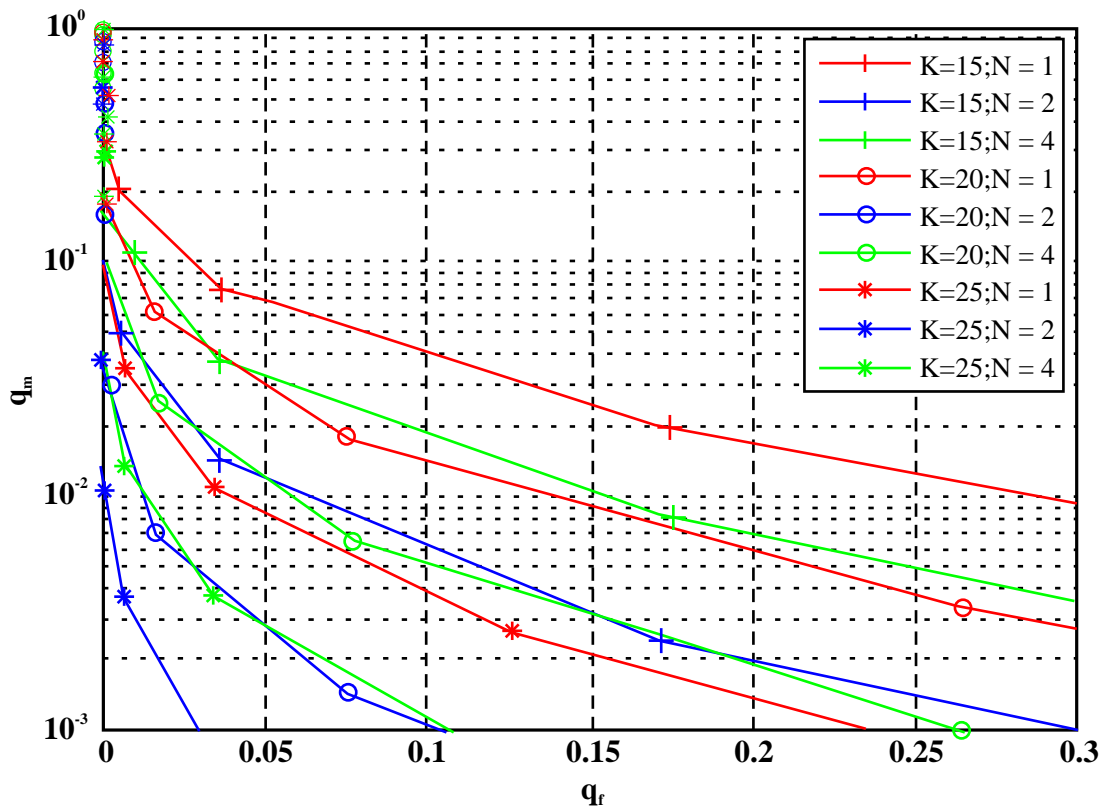


Figure 9: Impact of the number of transmitting sensors K and of the number hydrophone N on the CROC each with pulse duration $T_p = 1$ ms and $T_\theta = 12$ ms, operating at SNR= -25 of sampling frequency $F_s = 2$ kHz with $P_f=0.1$ and $P_m=0.4$.

Number of Sensors and Hydrophones: Now the figure. 9 explain the effect of the number of transmitting sensors (K) and of the number of hydrophone (N). The change with both K and N is evident. The decrease in global probability missed alarm from $q_m = 0.062$ to $q_m = 0.022$ at global probability of false alarm $q_f = 0.05$ and with $N = 1$ hydrophone at fusion centre can be achieved by moving from $K = 20$ to $K = 25$, this may asses the sensitivity with respect to K . The decrease in global probability missed alarm from $q_m = 0.022$ to $q_m = 0.018$ at global probability of false alarm $q_f = 0.05$ and with $K = 25$ hydrophone at fusion centre can be achieved by moving from $N = 1$ to $N = 2$, this may asses the sensitivity with respect to N . In addition, it is merit specify that the spatial diversity of the system is NK , i.e. the number of individual links. However, systems with the same product NK but different values for K and N undergo different performance, usually with the system having larger K and smaller N performing better.

Now, for the various value of SNR the performance loss between energy detector and optimal detector is demonstrated in figure 10. Actually, the curves related to the optimal detector have been acquired by utilizing the Max-Log approximation in E_q . (11). Such a detector, particularly Max-Log detector, has been appeared to perform nearly to the optimal detector because of the presence of exponential functions with large dynamic range i.e. without suffering of numerical instability. In order to assess the gap, it is merit seeing that energy detector and optimal detectors at a global probability of false alarm $q_f = 0.05$ and SNR = -25dB provide a global probability of missed detection of $q_m = 0.087$ and $q_m = 0.024$, respectively.

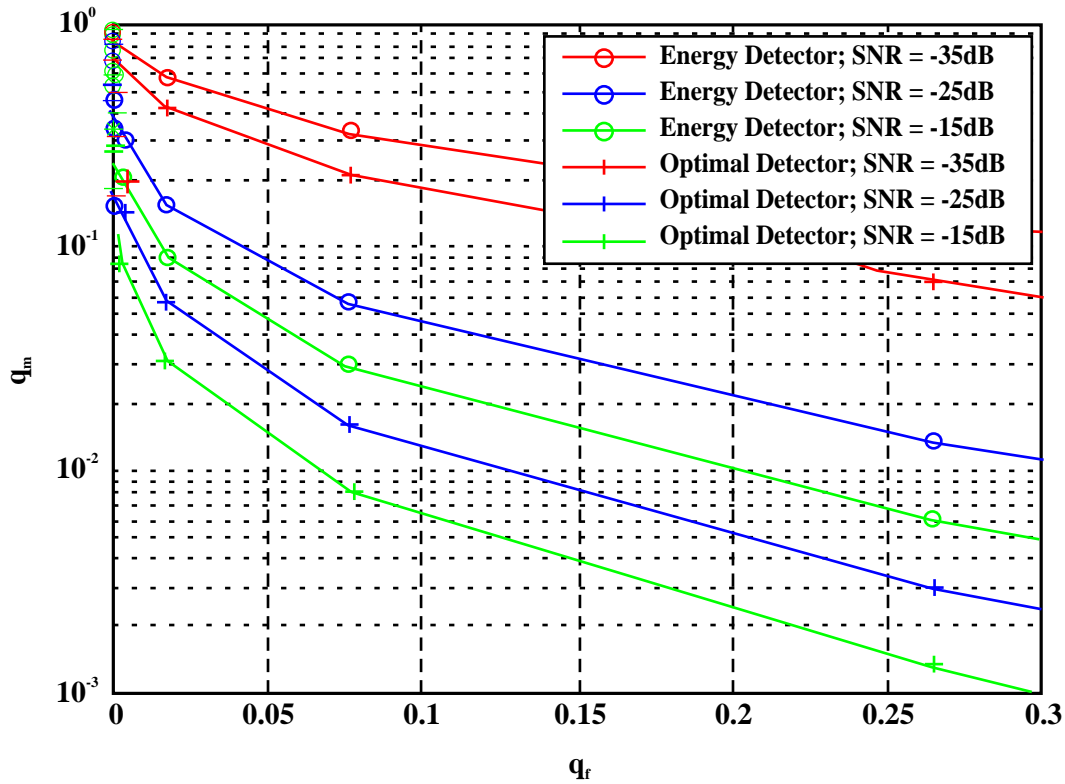


Figure 10: performance loss of the energy detector with respect to optimal detector with $K = 25$ transmitting sensor and of the number hydrophone $N = 1$ at fusion centre on the CROC each with pulse duration $T_p = 1$ ms and $T_0 = 12$ ms, operating at SNR= -25 of sampling frequency $f_s = 2$ kHz with $P_t = 0.1$ and $P_m = 0.4$.

Now, from the above result we conclude that on one hand energy detector accomplish extremely good performance, on another hand it also requires extremely low computational complexity and limited system knowledge (Lee et al., 2014). That is why diversity base decision fusion energy detector is certainly an interesting approach in underwater acoustic wireless sensor network, although it is suboptimal. It is worth remarking that:

- The integration time is depending on the particularly acoustic environment, which is roughly $T_0 = \tau_u + 3\tau_{rms}$.
- The pulse duration is depending on the sampling frequency $T_p = 1/f_s$
- Analytical classification regarding the numerous sensor and hydrophone and local performance is not easy, however outstanding performance can be attained even with the low quality of sensors and restricted number of transmit/receive elements.

Despite the fact that quantitative results are connected to a particular value that were assumed, we expect that the same qualitative results hold for a generic underwater environment.

Conclusion

In this paper we addressed the design of the sub-optimal rule, suitable for practical implementation for decision fusion task performed over a MMO channel in underwater sensor network. Underwater acoustic channels have been modeled with time-varying multipath. The overall performance of detector is extremely good with low computational complexity and limited system knowledge. The results show

that in realistic scenario even with low-quality of sensor this approach can be easily obtained.

References

- Akyildiz, F., Pompili, D., Melodia, T. 2005. Underwater acoustic sensor networks: Research challenges. *Ad Hoc Network*.3(3), 257–279.
- Chen, B., Jiang, R., Kasetkasem, T., Varshney, P. K. 2009. Channel aware decision fusion in wireless sensor networks. *IEEE Trans. Signal Process*, 52(12), 3454–3458.
- Berger, C. R., Guerriero, M., Zhou, S., Willett, P. 2009. PAC vs. MAC for decentralized detection using non-coherent modulation. *IEEE Trans. Signal Process*, 57(9), 3562–3575.
- Catipovic, J.A. 1990. Performance limitations in underwater acoustic telemetry. *IEEE J. Ocean. Eng*, 15(3), 205–216.
- Chen, B., Tong, L., Varshney, P.K. 2006. Channel-aware distributed detection in wireless sensor networks. *IEEE Signal Process. Mag.*, 23 (4),16–26.
- Chen, Y.S., Lin, Y.W. 2013. Mobicast routing protocol for underwater sensor networks. *IEEE Sensors J*, 13(2), 737–749.
- Ciuonzo, D., Romano, G., Salvo Rossi, P. 2012. Channel-aware decision fusion in distributed MIMO wireless sensor networks: Decode-and-fuse vs. decode-then-fuse. *IEEE Trans. Wireless Communication*, 11(8), 2976–2985.
- Ciuonzo, D., Romano, G., Salvo Rossi, P. 2013. Performance analysis and design of maximum ratio combining in channel-aware MIMO decision fusion. *IEEE Trans. Wireless Communication*, 12(9), 4716–4728.
- Ciuonzo, D., Romano, G., Salvo Rossi, P. 2015. Optimality of received energy in decision fusion over Rayleigh fading diversity MAC with non-identical sensors. *IEEE Trans. Signal Process*, vol. 61, no. 1, pp: 22–27.
- Guo, X., Frater, M. R., Ryan, M.J. 2009. Design of a propagation-delay tolerant MAC protocol for underwater acoustic sensor networks. *IEEE J. Ocean. Eng.*, 34(2), 170–180.
- Jordet, J.M., Stojanovic, M., Zorzi, M. 2010. On joint frequency and power allocation in a cross-layer protocol for underwater acoustic networks. *IEEE J. Ocean. Eng.*, 35(4), 936–947.
- Kanchumarthy, V. R., Viswanathan, R., Madishetty, M. 2008. Impact of channel errors on decentralized detection performance of wireless sensor networks: A study of binary modulations, Rayleigh-fading and non-fading channels, and fusion-combiners. *IEEE Trans. Signal Proces*, 56(5), 1761–1769.
- Kay, S.M. 1998. Fundamentals of Statistical Signal Processing: Detection Theory, Vol. 2. Englewood Cliffs, NJ, USA: *Prentice-Hall*.
- Kilfoyle, D.B., et al. 2005. Spatial modulation experiments in the underwater acoustic channel. *IEEE J. Ocean Eng.*, vol. 30, no. 2, pp: 406–415.
- Lanbo, L., Shengli, Z., Jun-Hong, C. 2008. Prospects and problems of wireless communication for underwater sensor networks. *Wireless Communication Mobile Commutating*, 8(8), 977–994.
- Lee J., Tepedelenlioglu, C. 2014. Distributed detection in coexisting large scale sensor networks. *IEEE Sensors J*, 14(4), 1028–1034.
- Lee, J., Tepedelenlioglu, C. 2017. Distributed detection in coexisting large scale sensor networks. *IEEE Sensors J*, 14(4), 1028–1034.
- Lei Schober, R. 2010. Coherent max-log decision fusion in wireless sensor networks. *IEEE Trans. Communication.*, 58(5), 1327–1332.

- Li, B., et al. 2009. MIMO-OFDM for high-rate underwater acoustic communications. *IEEE J. Ocean. Eng.*, 34(4), 634–644.
- Li, B., Zhou, S., Stojanovic, M., Freitag, L., Willett, P. 2008. Multicarrier communication over underwater acoustic channels with non-uniform Doppler shifts. *IEEE J. Ocean. Eng.*, 33(2), 198–209.
- Li, F., Evans, J.S., Dey, S. 2011. Decision fusion over non-coherent fading multi-access channels. *IEEE Trans. Signal Process.*, 59(9), 4367–4380.
- Liao, W.H., Huang, C.C. 2012. SF-MAC: A spatially fair MAC protocol for underwater acoustic sensor networks. *IEEE Sensors J.*, 12(6), 1686–1694.
- Nordenvaad, M.L., Oberg, T. 2006. Iterative reception for acoustic underwater MIMO communications in *Proc. IEEE OCEANS Conference*, 1–6.
- Park M. K., Rodoplu, V. 2007. UWAN-MAC: An energy-efficient MAC protocol for underwater acoustic wireless sensor networks. *IEEE J. Ocean. Eng.*, 32(3), 710–720.
- Park, J., Kim, E., Kim, K. 2010. Large-signal robustness of the Chair–Varshney fusion rule under generalized-Gaussian noises. *IEEE Sensors J.*, 10(9), 1438–1439.
- Roy, S., Duman, T., Ghazikhanian, L., McDonald, V., Proakis, J., Zeidler, J. 2004. Enhanced underwater acoustic communication performance using space-time coding and processing. in *Proc. IEEE OCEANS Conference*, 1, pp: 26–33.
- Song, X., Willett, P., Glaz, J., Zhou, S. 2012. Active detection with a barrier sensor network using a scan statistic. *IEEE J. Ocean. Eng.*, 37(1), 66–74.
- Sozer, E.M., et al. 2000. Underwater acoustic networks. *IEEE J. Ocean Eng.*, 25(1), 72–83.
- Stojanovic, M., Preisig, J. 2009. Underwater Acoustic Communication Channels: Propagation Models and Statistical Characterization. *IEEE Communications Magazine*.
- Van P.A., Walree, Otnes, R. 2013. Ultra-wide band underwater acoustic communication channels. *IEEE J. Ocean. Eng.*, 38(4), 678–688.
- Van Walree, P.A., Leus, G. 2009. Robust underwater telemetry with adaptive turbo multiband equalization. *IEEE J. Ocean. Eng.*, 34(4), 645–655.
- Varshney, P.K. 1996. Distributed Detection and Data Fusion. New York, NY, USA: *Springer-Verlag*.
- Wang, Z., Zhou, S., Giannakis, G.B., Berger, C.R., Huang, J. 2012. Frequency-domain oversampling for zero-padded OFDM in underwater acoustic communications. *IEEE J. Ocean. Eng.*, 37(1), 14–24.
- Xu, Z., Huang, J., Zhang, Q. 2013. Power constrained partially coherent distributed detection over fading multiaccess channels. *IEEE Sensors J.*, 13(7), 2729–2736.
- Yang, T.C. 2007. A study of spatial processing gain in underwater acoustic communications. *IEEE J. Ocean Eng.*, 32(3), 689–709.
- Zhang, G., Dong, H. 2011. Spatial diversity in multichannel processing for underwater acoustic communications. *Ocean. Eng.*, 38(14–15), 1611–1623.
- Zhang, G., Dong, H. 2011. Experimental assessment of a multicarrier underwater acoustic communication system. *Appl. Acoust.*, 72(12), 953–961.
- Zhang, G., Dong, H. 2012. Experimental demonstration of spread spectrum communication over long range multipath channels. *Appl. Acoust.*, 73(9), 872–876.
- Zhang, S., Li, D., Chen, J. 2013. A link-state based adaptive feedback routing for underwater acoustic sensor networks. *IEEE Sensors J.*, 13(11), 4402–4412.
- Zorzi, M., Casari, P., Baldo, N., Harris, A.F. 2008. Energy-efficient routing schemes for underwater acoustic networks. *IEEE J. Sel. Areas Commun.*, 26(9), 1754–1766.